ELSEVIER

Materials Chemistry and Physics 43 (1996) 166–172

MATERIALS CHEMISTRY AND PHYSICS

Characterization of anodic aluminum oxide film and its application to amorphous silicon thin film transistors

C.W. Liang[a], T.C. Luo[a], M.S. Feng[b,*], H.C. Cheng[a], David Su[c]

[a]*Department of Electronics Engineering, Institute of Electronics, and National Nano Device Laboratory, National Chiao Tung University, 1001 Ta Hsueh Road, Hsinchu 30049, Taiwan, ROC*

[b]*Institute of Materials Science and Engineering, and National Nano Device Laboratory, National Chiao Tung University, 1001 Ta Hsueh Road, Hsinchu 30049, Taiwan, ROC*

[c]*Unipac Optoelectronic Inc., Science-Based Industrial Park, Hsinchu, Taiwan, ROC*

Received 8 February 1995; revised 24 May 1995; accepted 26 May 1995

Abstract

Al_2O_3/SiN_x double-layered dielectric films suitable for large-size amorphous silicon thin film transistor liquid crystal displays (a-Si:H TFT LCD) have been prepared by anodization and plasma enhanced chemical vapor deposition (PECVD). Al_2O_3 films were formed at various pH values and volume ratio of water ($H_2O\%$) in the electrolyte. The optimal quality of Al_2O_3 film was achieved at pH = 6 and $H_2O\% = 30$. These high-quality Al_2O_3 films have denser structure, lower etching rate (90 Å min^{-1}) and smooth surface morphology after etching. The capacitors made of the anodization show a breakdown field as high as 7.8 MV cm^{-1} and a low leakage current density of 10 nA cm^{-2} at a dielectric field of 3 MV cm^{-1}. Furthermore, a-Si:H TFTs with Al gate and different gate dielectrics (Al_2O_3/SiN_x and SiN_x) were also fabricated and evaluated. The TFTs with Al_2O_3/SiN_x double-layered gate dielectric provide better performances, such as the smaller threshold voltage (1.76 V), improved subthreshold swing (1.0 V dec^{-1}), and lower off-current (3.8 PA) than those of the device with single SiN_x film.

Keywords: Anodization; Al_2O_3; Amorphous silicon; Thin film transistor

1. Introduction

In recent years, the hydrogenated amorphous silicon thin film transistors (a-Si:H TFTs) have been receiving extensive attentions owing to their critical roles in large-area integration, such as the matrix addressing elements of liquid crystal displays [1], linear arrays of image sensors [2], and linear arrays for driving page-width printers [3].

Recently, the development of TFT-LCD has focused on the large area issues. One of the most serious problems is the address delay and distortion caused by the resistance and capacitance of the gate bus lines. Various materials such as Cr [4], Ti [5], MoTa [6], or Ta [7], have been proposed as the candidates for the gate bus lines of TFT-LCDs. However, the resistances of these metals are not low enough to meet the requirements of large area (~14-in. diagonal) TFT-LCD. In this respect, aluminum is a material with a resistivity as low as 4 $\mu\Omega$-cm, and hence it is appropriate for the realization of large-size panel displays. Unfortunately, the Al film is prone to the formation of hillocks during the heating process, which will cause serious interlayer short defects between the gate bus and data lines due to the intrinsic stress existing between the aluminum electrode and the gate insulator (i.e., silicon nitride, SiN_x) [8]. Accordingly, an Al_2O_3 film formed by anodization was introduced between the aluminum and SiN_x films to suppress hillock formation. It has been demonstrated that the defect density and gate resistance of a-Si:H TFTs can be significantly reduced as long as the hillock formation is successfully eliminated by the application of $Al/Al_2O_3/SiN_x$ structures [9].

In this study, the anodized Al_2O_3 films, prepared under various conditions, are characterized in detail. Our analyses include the observation of the scanning-

* Corresponding author. Tel.: +886 35 712121 ext. 55301; Fax: +886 35 724727.

SSDI 0254-0584(95)01619-6

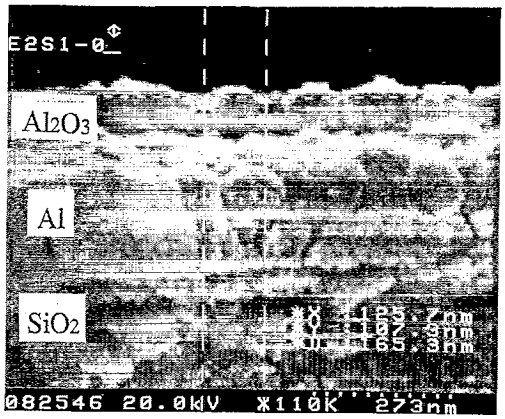

Fig. 1. Cross-sectional SEM micrograph of the Al_2O_3 prepared by the anodic oxidation method.

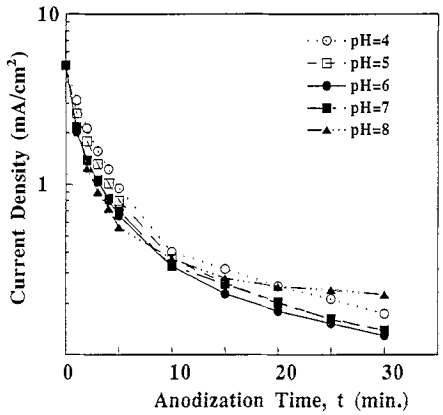

Fig. 3. Current density versus anodization time at 100 V anodization voltage showing the current density decreases as the anodization time increases at various pH values.

electron microscope (SEM), the measurement of etching rate and the evaluations of the I-V characteristics, electrical breakdown field, leakage current density and time-zero-dielectric-breakdown (TZDB) of the metal-insulator-metal (MIM) structure. In addition, the transfer characteristics of the a-Si:H TFTs with different gate dielectrics will be investigated and compared.

2. Experiment

Silicon wafers with 5000 Å thermal oxide were used as the substrate, on which 3000 Å aluminum film was deposited by thermal evaporation. The Al_2O_3 was grown by an anodization system as described elsewhere [10]. The effects of the pH value and the water to ethylene glycol ratio on the growth of anodic film were investigated. The anodization solution consisted of 10 g of tartaric acid, 300 g of water and 400 ml of ethylene glycol. It was buffered with a 28% aqueous solution of ammonia for the adjustment of the pH value in the range of 4 to 8. In the initial stage of anodization, the applied voltage was increased continuously to maintain a constant current density (constant-current mode). Then, it was kept at a predetermined level for a period, during which the current density began to decay (constant-voltage mode). As the lower limit of the anodization current was reached, the power was switched off and the anodization was completed. The substrate on which the Al_2O_3 was grown was then removed from the electrolytic bath and dipped in pure ethylene glycol for a few minutes, followed by the rinse of doubly distilled water. Afterwards, the Al_2O_3 film was annealed in N_2 ambient at 300 °C. The thicknesses of the Al_2O_3 films are measured by cross-sectional SEM view and ellipsometer.

The metal-insulator-metal (MIM) capacitors were fabricated by the following process. A 5000 Å-thick aluminum film was deposited on a silicon substrate with 5000 Å SiO_2. After the anodization and annealing processes described above, an aluminum pattern with an area of 2×10^{-3} cm^2 was deposited onto the Al_2O_3 film to form the MIM structure.

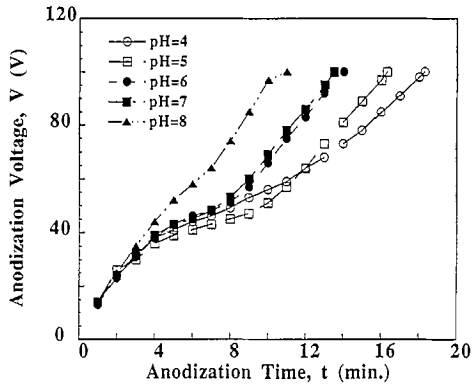

Fig. 2. Anodization voltage versus anodization time for various pH values in the anodization bath.

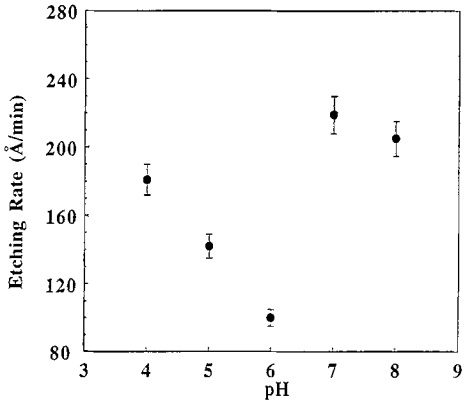

Fig. 4. Effect of pH value in the electrolyte on the etching rate of Al_2O_3 films.

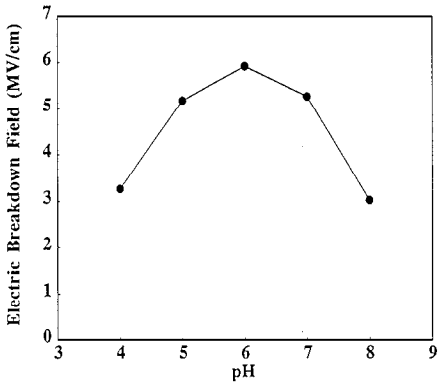

Fig. 5. Electrical breakdown field of Al_2O_3 film grown under various pH values. An optimal electrical breakdown field characteristics is observed at pH = 6.

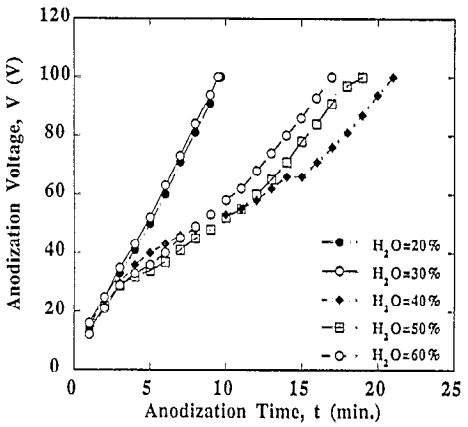

Fig. 6. Anodization voltage versus anodization time for various H_2O% in the electrolyte.

The a-Si:H TFTs with inverted staggered structure were also prepared in this work. An aluminum gate with thickness of 3000 Å was deposited on substrate, and the Al_2O_3 layer of 1000 Å was grown by the anodization process. The gate electrode, with a layer of Al_2O_3, was defined by the standard photolithography technology. After the formation of the gate, a silicon nitride film of 2200 Å and an a-Si:H film of 2500 Å were deposited sequentially in a PECVD reactor. Limited by the PECVD reactor, the authors did not use the n^+ a-Si:H layer at the source/drain contacts. Following the patterning of the a-Si:H and SiN_x films, an aluminum film of 5000 Å was thermally evaporated and patterned to form the source/drain contacts. The channel length and width are 40 and 80 μm respectively.

For electrically characterizing the anodized Al_2O_3 layer, we evaluate the I-V characteristics and Time zero dielectric breakdown (TZDB) of our MIM capacitors. Meanwhile, the transfer characteristics of the fabricated a-Si:H TFTs were also inspected. Besides, the surface morphology of the Al_2O_3 film was examined by SEM.

3. Results and discussion

The layer configuration of the $SiO_2/Al/Al_2O_3$ structure was inspected by SEM. Fig. 1 demonstrates a typical scanning electron micrograph of the $SiO_2/Al/Al_2O_3$ structure ($SiO_2/Al/Al_2O_3$: 5000 Å/5000 Å/1073 Å). Obviously, the Al_2O_3 film has been successfully grown on the top surface of aluminum. It is well known that the thickness of the Al_2O_3 film is increased mainly in the period of constant current-density mode. The subsequent application of a constant voltage is meant to densify the oxide film by filling the voids and depressions formed in the previous constant-current stage [11]. Besides, the thickness of the Al_2O_3 films can be accurately controlled since it is proportional to the value of applied voltage. In this work, the proportionality factor is found to be about 12 Å V^{-1}.

The relations of the anodization voltage (V) to keep a constant current-density of 0.5 mA cm^{-2} versus the anodization time (t) with different pH values are shown in Fig. 2. As can be seen, the variation rates of the anodization voltage (dV/dt, which is proportional to the growth rate of the Al_2O_3 film) increase monotonically with pH value. It is because the concentration of O^{2-} ions in the anodization bath increases as pH value is increased. We also observe that the anodization current density of the sample grown at pH = 6, during the period of constant-voltage mode, shows the most rapid decay (see Fig. 3). It implies that the Al_2O_3 film grown at pH = 6 exhibits the most condensed structure, as compared with the films grown at different pH values [12]. The quality of Al_2O_3 film can be revealed by the etching rate in the standard aluminum etchant (a mixture of HPO_3, HNO_3, CH_3COOH, and H_2O). As shown in Fig. 4, the etching rate reaches a local minimum at pH = 6. This is consistent with the results shown in Fig. 3. The authors' inference about the film quality can be further confirmed by the dependence of the breakdown field (E) of the MIM capacitors on the electrolyte pH

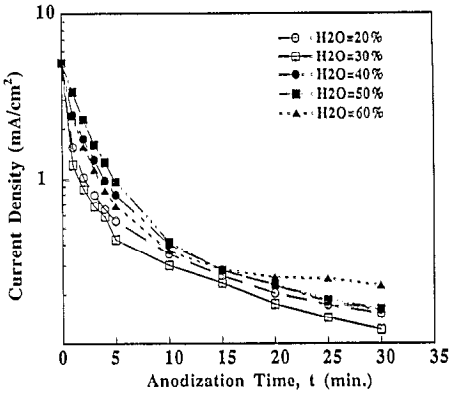

Fig. 7. Current density versus anodization time at 100 V anodization voltage showing the current density decreases as the anodization time increases at various H_2O% in the electrolyte.

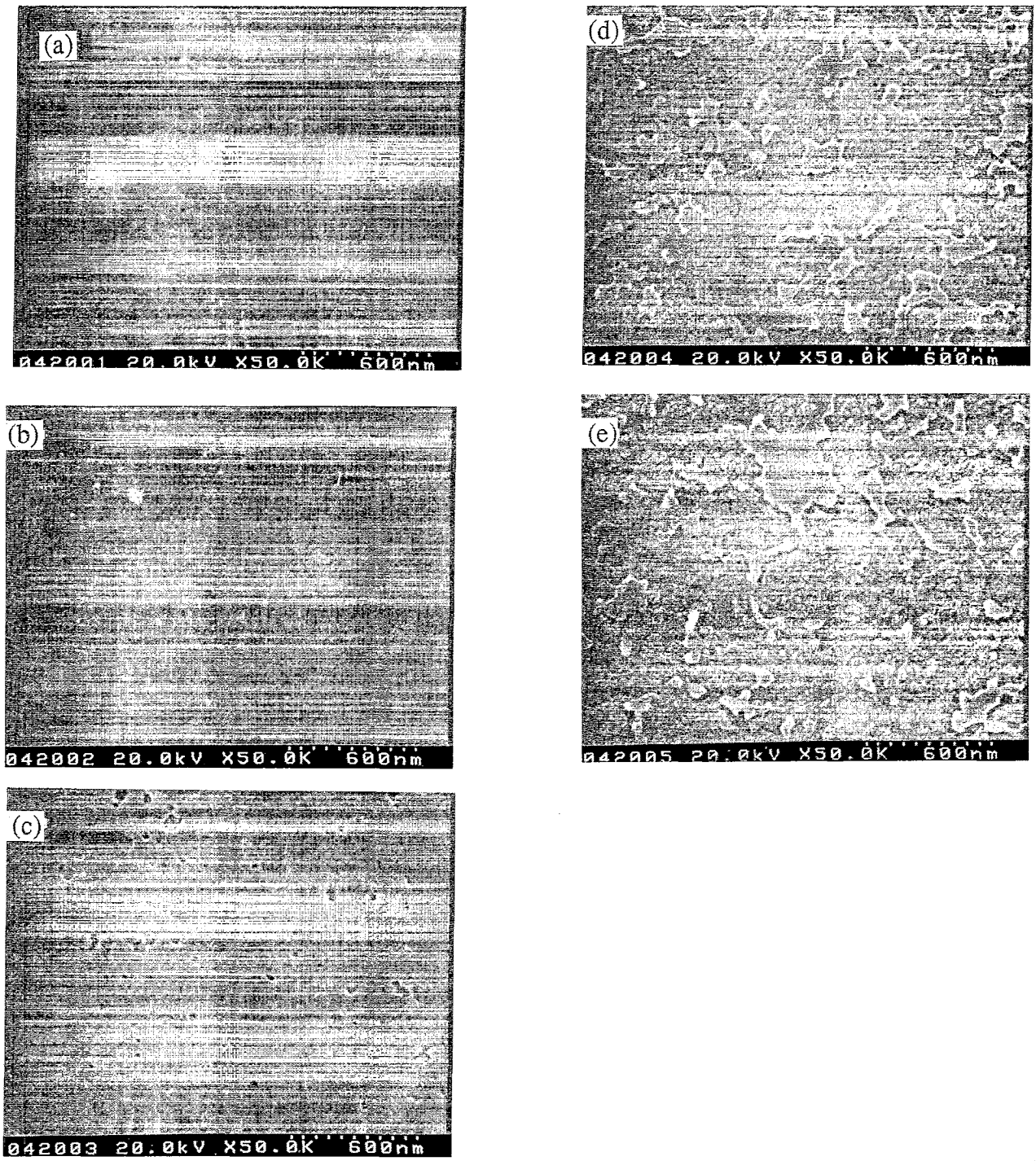

Fig. 8. SEM surface morphologies of Al_2O_3 films after etching, which were formed at various $H_2O\%$ in the electrolyte: (a) $H_2O\% = 20$, (b) $H_2O\% = 30$, (c) $H_2O\% = 40$, (d) $H_2O\% = 50$, (e) $H_2O\% = 60$.

value, as shown in Fig. 5. It is noticed that a maximum breakdown field occurs at pH = 6. To sum up, we conclude that the optimum pH value of the electrolyte for the growth of anodized Al_2O_3 is 6.

Next, we consider another important parameter in the anodization process: the water contents in the electrolyte. In general, the electrolyte meanly consists of three components: (i) glycol, (ii) water, and (iii) a suitable acid. Water plays the role of the anodic oxidant for Al, while the acid is added to guarantee successful ionic conduction in the electrolyte. The selection of the acid is not trivial since it might cause some disastrous effects on the oxide growth, such as strong in-situ oxide dissolution if improperly selected. As for component (i), ethylene glycol has been claimed to be capable of reducing the limiting current density, the solubility of the initial anodic products and the transport rate of these products [13].

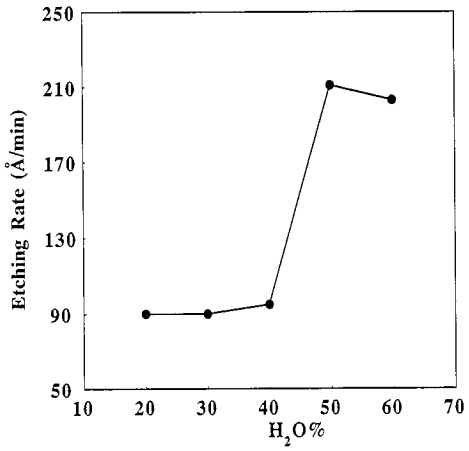

Fig. 9. Effect of $H_2O\%$ in the anodization solution on the etching rate of Al_2O_3 films.

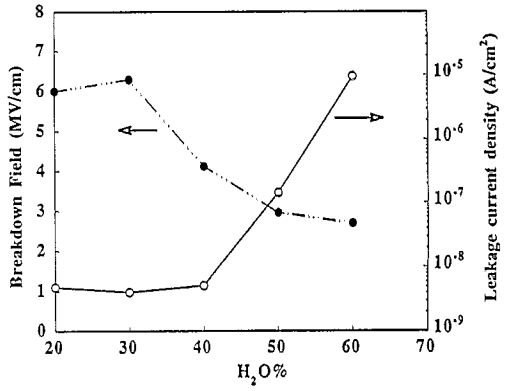

Fig. 10. Leakage current density and breakdown field characteristics of MIM capacitor with Al_2O_3 layer formed at various $H_2O\%$ in the electrolyte.

Fig. 6 shows the effect of the water ratio ($H_2O\%$) in the electrolyte on the growth and quality of the anodized oxide, in which the anodization voltage versus the anodization time with a constant current density of 0.5 mA cm^{-2} was monitored. It was found that the anodization of aluminum is very sensitive to the ratio of H_2O in the electrolyte. The anodization solution was prepared by mixing 5 g of tartaric acid and 100 g of water at first, and then diluted by ethylene glycol to satisfy the required volume ratio. It was also buffered with the aqueous solution of ammonia for pH value adjustment (pH = 6 in this case). As shown in Fig. 6, dV/dt, which is proportional to the growth rate of Al_2O_3, decreases with $H_2O\%$ with $H_2O\% \leqslant 40$. However, it becomes an increasing function of $H_2O\%$ afterwards. The decrease of the growth rate by $H_2O\%$ with $H_2O\% \leqslant 40$ is due to the increased dissolution rate. Additionally, we observed that the anodization current density decreased more rapidly for the sample grown at $H_2O\% = 30$ than the others in the constant voltage stage (100 V), as can be seen in Fig. 7. Similarly, it indicates that the better quality of the Al_2O_3 films was formed at $H_2O\% = 30$. Moreover, the surface morphologies of the Al_2O_3 films were also inspected by SEM. Fig. 8 clearly demonstrates that there are many pits on the samples prepared by the electrolyte with $H_2O\% = 60$ (Fig. 8(e)) and $H_2O\% = 50$ (Fig. 8(d)), and the pit density is considerably reduced with $H_2O\% \leqslant 40$. Actually, there is almost no pitting on the Al_2O_3 films with $H_2O\% = 20$ (Fig. 8(a)) and 30 (Fig. 8(b)). This can definitely be attributed to the dominance of the barrier-type films at $H_2O\% \leqslant 30$. The reason for the formation of denser structure by the addition of glycol could be either a decrease in the solubility of the initial anodic products, or a reduction in the transport rate of such products, or both, leading to an easier establishment of supersaturation [8]. The etching rate of the Al_2O_3 film was found to be closely related to its surface morphology, as seen in Fig. 9. Evidently, the etching rate of Al_2O_3 is hardly affected by $H_2O\%$ with $H_2O\% \leqslant 40$, and it increases abruptly as $H_2O\%$ becomes larger. Therefore, the strong dependence of the quality of Al_2O_3 film on the ratio of H_2O in the electrolyte can never be overlooked.

As for the electrical performances, the authors investigated the effect of $H_2O\%$ on the leakage current and the breakdown field of the MIM capacitors with the anodized Al_2O_3, and the results are shown in Fig. 10. The breakdown field decreases as $H_2O\%$ increases, while the leakage current exhibits an opposite tendency. It agrees with the previous results obtained from various analyses. To summarize the experimental results described above, we conclude that pH = 6 and $H_2O\% = 30$ are the optimal conditions for the growth of Al_2O_3 in the anodization process.

The operational principles of a-Si:H TFTs are quite different from those of crystalline MOSFETs because of the distinguishing properties of the a-Si:H film. First of all, the n-channel a-Si:H TFTs operate in accumulation mode since the Fermi level of intrinsic a-Si:H is about 0.2-0.3 eV above the midgap in general. Besides, the characteristics of a-Si:H TFTs are determined by the localized states existing in the band gap. In addition to the intrinsic properties of a-Si:H film, the characteristics of a-Si:H TFTs are also sensitive to the defect states in the gate dielectric and the interface property. It has been reported that the interface states between a-Si:H and SiN_x with an Al gate will be affected by hillocks formed between the Al and SiN_x layers. Therefore, the Al_2O_3 film, sandwiched between aluminum and SiN_x, can be grown by the above anodization technology to prevent the hillock formation, and the effects of the resultant bilayer structure of Al_2O_3/SiN_x on the performance of a-Si:H TFTs can be investigated. A comparison of the transfer curves of a-Si:H TFTs with different dielectric structures is shown in Fig. 11. The devices were biased at $V_d = 10$ V, where V_d is the drain-to-

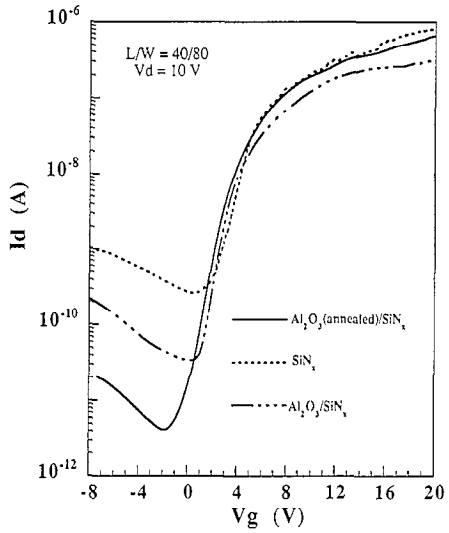

Fig. 11. Transfer characteristics of a-Si:H TFTs with three different gate dielectrics: Al_2O_3(annealed)/SiN_x, SiN_x, and Al_2O_3/SiN_x ($V_d = 10$ V).

source voltage. The higher on-current of a-Si:H TFT with monolayer dielectric SiN_x is due to its larger dielectric capacitance. However, the off-current of a-Si:H TFT with single SiN_x is larger than that with Al_2O_3/SiN_x. It can be easily understood by recalling the high densities of pinholes in the SiN_x film deposited by PECVD and hillocks in aluminum, both of which provide an efficient path for electrons to flow from gate to drain under negative gate bias. In this respect, the role of the Al_2O_3 film can be emphasized since it works as a protective layer against hillock formation and thus the off-current is lowered accordingly. Besides, the lack of an n^+ a-Si:H layer also results in higher off-current (hole current) in the negative gate bias region. The threshold voltages (V_t) and subthreshold swings of the a-Si:H TFTs with different gate dielectrics are listed in Table 1. The threshold voltages of a-Si:H TFTs are sensitive to the density of interfacial charges (Q_{it}) as well as the trapped-charge density (Q_t) in gate insulator. The threshold shift (ΔV_t) caused by the addition of Q_{it} and Q_t can be calculated by [14]

$$\Delta V_t = -\left[\frac{Q_{it} + Q_t}{C_{ins}}\right] \tag{1}$$

where C_{ins} is the gate capacitance per unit area. Then, the larger threshold voltage of the TFT with the single layer of SiN_x can be ascribed to the higher interfacial charge density (Q_{it}) than that with the bilayer of Al_2O_3/SiN_x, because the penetration of the hillocks formed between Al and SiN_x layers into SiN_x will lead to a rough a-Si:H/SiN_x interface and a higher Q_{it} eventually. Furthermore, the subthreshold swing S, which is defined as the inverse slope of the I-V characteristics in a semi-log plot, $dV_g/d(\log I_d)$, is directly related to the ability of V_g to shift the Fermi level against the retardation of band-gap states. The interface-state density Ni can be roughly estimated by [15]

$$N_i = \frac{\varepsilon K_{ins}}{q d_{ins}}\left(S\frac{q}{\ln 10 kT} - 1\right) \tag{2}$$

where ε is the permittivity of free space, T is the measured temperature, k is the Boltzmann's constant, d_{ins} is the thickness of gate insulator, and K_{ins} is the dielectric constant of gate insulator. As listed in Table 1, the TFT with Al_2O_3/SiN_x gate dielectric shows better subthreshold characteristics and N_i is estimated to be 2.38×10^{12} cm^{-2}. On the other hand, N_i of the TFT with monolayer of SiN_x is about 4.12×10^{12} cm^{-2}. The improvement of the interface quality by the application of anodized Al_2O_3 is quite evident. The performance of the TFTs with the bilayer of Al_2O_3/SiN_x can be further improved by annealing treatment. The as-grown Al_2O_3 film will inevitably contain many water-related trapping centres, which can be eliminated by the annealing treatment. Characteristically, the performance of TFTs discussed in this paper are inferior to the conventional one's (i.e., on-current less than 1 μA, S larger than 1 V dec^{-1}, and mobility around 0.3 cm^2/S-V). The lack of an n^+ a-Si:H layer is responsible for this, owing to the high contact resistance between the source/drain and active layer.

4. Conclusions

It has been successfully demonstrated that high-quality and good-uniformity Al_2O_3 insulating films can be grown by an anodization technique in which the tartaric acid solution buffered by ammonia and diluted with ethylene glycol is selected to be the electrolyte. The film quality of the anodized Al_2O_3 films strongly depends on the pH and H_2O% values in the electrolyte.

Table 1
Performance of a-Si:H TFTs with various gate dielectrics

Gate dielectric	V_t (V)	Subthreshold swing (V dec^{-1})	I_{on}/I_{off} ratio	I_{on} (μA) at $V_g = 20$ V	I_{off} (pA)
Al_2O_3/SiN_x (annealed)	1.76	1.00	2×10^5	0.66	3.8
Al_2O_3/SiN_x	1.89	1.05	1×10^5	0.32	33.5
SiN_x	2.55	1.69	3×10^4	0.81	260.5

After carefully evaluating the leakage current, the breakdown field, the etching rate and the surface morphologies of the Al_2O_3 grown at various conditions, we find that the optimal recipe for the electrolyte is pH 6 and $H_2O\% = 30$. The electrical characteristics of the a-Si:H TFTs with three different gate dielectrics, Al_2O_3(annealed)/SiN_x, Al_2O_3/SiN_x, and SiN_x, were compared, too. It was found that the a-Si:H TFT with a bilayer structure of Al_2O_3(annealed)/SiN_x showed the best performances, and hence the anodized Al_2O_3 is an efficient protective layer against hillock formation. We would like to emphasize that Al is adequate for realizing large-size LCDs due to its extremely low resistivity, as long as the problem of hillock formation can be solved by using anodized Al_2O_3.

Acknowledgement

This work has been sponsored by the National Science Council of the ROC under the contract NSC 79-0404-E009-001.

References

[1] A.J. Snell, K.D. Mackenzie, W.E. Spear, P.G. Le Comber and A.J. Hughes, *Appl. Phys.*, *24* (1981) 357.
[2] H. Ito, T. Suzuki, Y. Nishihara, Y. Sakai, T. Ozawa and S. Tomiyama, *Mater. Res. Soc. Symp. Proc.*, *95* (1987) 437.
[3] L.E. Fennell, M.J. Thompson, H.C. Tuan and R. Weisfield, *Conf. Rec. Int. Display Research Conf.*, 1988, p. 167.
[4] H. Tanaka, S. Motte, M. Hoshino, K. Takahashi, M. Ohta, T. Sakai and T. Yamazaki, *SID 87 Digest*, 1987, p. 140.
[5] D.E. Castleberry and G.E. Possin, *SID 88 Digest*, 1988, p. 232.
[6] M. Dohjo, T. Aoki, K. Suzuki, M. Ikeda, T. Higuchi and Y. Oana, *SID 88 Digest*, 1988, p. 330.
[7] M. Katayama, H. Morimoto, S. Yasuda, T. Takamatu, H. Tanaka and M. Hijikigawa, *SID 88 Digest*, 1988, p. 310.
[8] W.Z. Manookian and J.I.B. Wilson, *IEE Proc.*, *133*(I) (1986) 153.
[9] T. Tsukada, *Mater. Res. Soc. Proc.*, *284* (1993) 371.
[10] C.F. Yeh, J.Y. Cheng and J.H. Lu, *Jpn. J. Appl. Phys.*, *32* (1993) 2803.
[11] S.G. Byeon and Y. Tzeng, *J. Electrochem. Soc.*, *123*(10) (1988) 2452.
[12] J.O'M Bockris (ed.), *Modern Aspects of Electrochemistry*, Vol. 2., Butterworths, London, 1959, p. 262.
[13] S. Ahmad and R. Singh, *Thin Solid Films*, *74* (1980) 165.
[14] S. Luan and G.W. Neudeck, *J. Appl. Phys.*, *68* (1990) 3445.
[15] A. Rolland, J. Richard, J.P. Kleider and D. Mencaraglia, *J. Electrochem. Soc.*, *140* (1993) 3679.